On the modal response of mobile cables

Charlélie Bertrand, Chloé Plut, Claude-Henri Lamarque, Alireza Ture Savadkoohi

On the modal response of mobile cables

Bertrand C.*, Plut C.*, Lamarque C.-H.*, Ture Savadkoohi A.*

December 2019

Abstract

The paper presents methodologies for tracing modal responses of a translating cable. Governing system equations are obtained based on perturbation of the response around the stationary position of the translating catenary. Then, after separation of spatio-temporal system variables, a multiple scale method is endowed for treatment of equations in space. Frequencies and mode shapes of the system are detected by imposing solvability conditions on the system equations and/or via expansion of system variables in the form of Fourier series accompanied by imposing the existence of non-trivial solutions. Finally, obtained results are confronted with those which are obtained by finite difference method.

Keywords: Translating catenary, Modes and frequencies, Multiple Scale Method, Finite Difference Method

Contents

*Univ Lyon, ENTPE, LTDS UMR CNRS 5513, Rue Maurice Audin 69518 Vaulx-en-Velin Cedex, France

1 Introduction

Cables are used in many fields of engineering applications because of their different range of possible behaviors and their capability in covering large distance space. Many engineering designs in the domain of cables rely on the work of Irvine [1]. However, cable dynamics is still a domain of high interest since these elements are subjected to intrinsic and external nonlinearities, for instance when subjected to the wind [2] or temperature loads [3]. The literature in cable dynamics is quite extensive. For example, some works focused on singular effects due to moving oscillators [4], beam-cable systems [5, 6] and various topics in their nonlinear vibrations [7]. Some comprehensive formulations of cable theory are presented in [8] which provide enough tools to model the behavior of a cable in a given context.

One of ewamples of systems based on the cable mechanics is translating cables because of their common use in transportation or engineering process. The equation of motion for a translating catenary have been studied from the mid-nineteenth century started by Skutch [9] who showed the influence of the translating velocity on the frequencies of a rope hanging between ideal supports. Meanwhile, few works give a full methodology to compute the mode shapes and frequencies of a translating elastic catenary. Simpson [10] provide analytical solutions to obtain different profiles of a small-sag catenary, while Triantafyllou [11] proposed a pseudo-analytical method to detect behaviros of the translating catenary problem using the WKB technique [12]. Robust design of translating cables demands a correct modelling of their behaviors including nonlinear terms. O'Reilly and Varadi [13] modeled a three-dimensionnal behavior of a translating cable. Some works were investigated the influence of the boundary conditions and the influence of the length variation of a translating string on its response [14, 15].

A method of multiple scales have been endowed by Warminski and al. [16] to trace the bifurcations of a reduced-order model accounting for cable dynamics. Ferreti and al. [17] take into account for the galopping phenomenon occuring in an iced cable.

The need for a full and detailed methodology to derive the equation of motions for a translating catenary, to compute its mode shapes and to better understand its nonlinear response and its stability are of deep interest for further works. In this paper, the governing equations are derived from Eulerian viewpoint around a stationary position and are treated after the separation of spatio-temporal variables. We introduce two possibilities (based on pure analytical and analytic-numerical approaches) for predicting modal characteristics, i.e. frequencies and mode shapes, which give clear insight about the influences of system parameters, such as the velocity of the translation, on its detected dynamics.

Organisation of the paper is as it follows: governing equations are derived as a dynamic perturbation of the stationary configuration of an inextensible catenary in section (2); After separation of space and time variables in section (3), a space multiple scale method (SMSM) [18] is endowed to split the responses of the system into two different space scales; Two methods are proposed in section (4) to compute frequencies and modes for this system; Pros and cons of each possible method are then discussed in conclusion (5).

2 The model of the system and its governing equations

In this section, governing equations of a translating cable supplemented by its compatibility conditions are derived based on the Eulerian viewpoint.

2.1 The stationary position

We consider a cable with the mass per length and linear weight as m and w, respectively. The rigidity is denoted as EA where E is the Young modulus and A stands for the cross section of the cable. This cable is moving with an axial velocity as V between two ideal supports located at the curvilinear abscissa $s = 0$ and $s = L$. As the dynamics of the system is investigated in an eulerian viewpoint, the material derivative of an arbitrary scalar function f subjected to a tangential translation V (causing a convection of the curvilinear abscissa) is given by [11]:

$$\frac{\mathrm{D}}{\mathrm{D}t}\{f\} = \frac{\partial f}{\partial t} + \mathrm{V}\frac{\partial f}{\partial s} \tag{1}$$

Under the use of this derivative operator, we introduce a pure translational motion along the curvilinear abscissa for an established regime. Moreover, this velocity is assumed to be constant and homogeneous. Here, the local

influence of the elasticity is neglected for the equilibrium and elasticity effects can be obtained, as derived in [13]. We denote the static tension and static angle of the cable at the abscissa s as $\widetilde{T}_{\mathrm{S}}$ and $\widetilde{\Phi}_{\mathrm{S}}$, respectivley. The equations of motion are derived in a local basis $(\underline{t}, \underline{n})$ where $\underline{t}$ and $\underline{n}$ stand for the unit tangent and unit normal vectors respectively (see Fig.(1)). Considered system is illustrated by Fig.(1). Very general equations of the motions are derived by O'Reilly and Varadi [13] which can be reduced to presented equations by Triantafyllou [11] under some simplifying assumptions. The equations for stationary position (depicted in Fig.(1)) are given by:

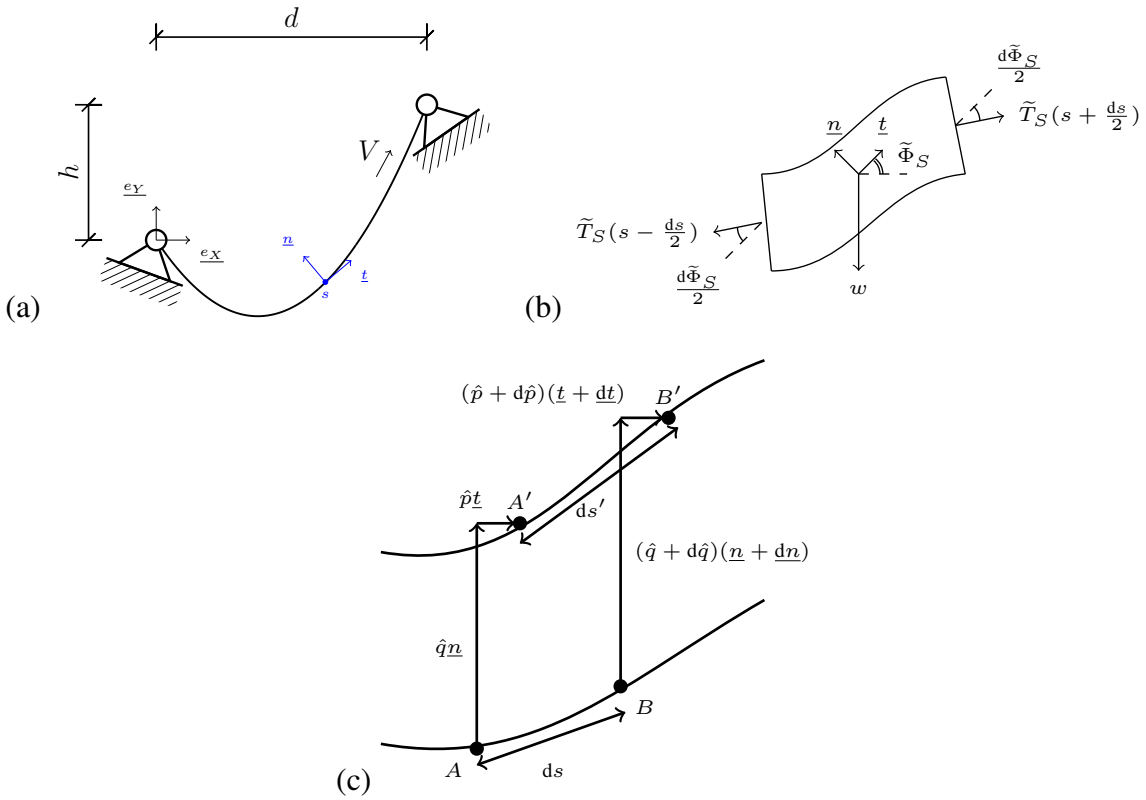

Figure 1: Representation of the system under consideration: (a) Translating catenary located between two ideal supports at stationary position; (b) Local equilibrium of the cable represented in the local referential; (c) Dynamic strain of the curvilinear domain of length ds delimited by points A and B during the motion of the cable

$$\underline{t} \qquad w \sin \widetilde{\Phi}_{\mathrm{S}} = \frac{\mathrm{d}\widetilde{T}_{\mathrm{S}}}{\mathrm{d}s} \tag{2}$$

$$\underline{n} \qquad w \cos \widetilde{\Phi}_{\mathrm{S}} = \left(\widetilde{T}_{\mathrm{S}} - m\mathrm{V}^2\right) \frac{\mathrm{d}\widetilde{\Phi}_{\mathrm{S}}}{\mathrm{d}s} \tag{3}$$

After some mathematical manipulations on Eqs.(2) and (3), it can be shown that:

$$\widetilde{T}_{\mathrm{S}} = \widetilde{T}_a \left(1 + \frac{w}{\widetilde{T}_a} \sin \widetilde{\Phi}_a (s - s_a) + \frac{1}{\widetilde{T}_a} \frac{(w \cos \widetilde{\Phi}_a)^2}{2\left(\widetilde{T}_a - m\mathrm{V}^2\right)} (s - s_a)^2\right) + \mathcal{O}((s - s_a)^3) \tag{4}$$

$$\frac{\mathrm{d}\widetilde{\Phi}_{\mathrm{S}}}{\mathrm{d}s} = \frac{w \cos \widetilde{\Phi}_a}{\widetilde{T}_a - m\mathrm{V}^2} - \frac{w^2 \sin(2\widetilde{\Phi}_a)}{\left(\widetilde{T}_a - m\mathrm{V}^2\right)^2} (s - s_a) + \mathcal{O}((s - s_a)^2) \tag{5}$$

where s_a is used as a reference point along the span of the cable and $(\widetilde{T}_a, \widetilde{\Phi}_a)$ are the values of the static tension and static angle at $s = s_a$. This expansion of the two static quantities are possible for every open domain without

singularities. The latter is assumed to be true in further developments.
In the next section, we will derive dynamic equilibrium state around the static state defines in Eqs.(4) and (5).

2.2 Dynamic equilibrium

We denote $\hat{p}$ and $\hat{q}$ as the displacement in the local directions of $\underline{t}$ and $\underline{n}$ vectors, respectively. We use the same methodology as for the static configuration to derive governing equations of the system. However, we introduce a dynamic perturbation around the static configuration which is clarified in Eqs.(4) and (5). Then we consider $\widetilde{T}_{\mathrm{S}} + \widehat{T}_{\mathrm{D}}$ and $\widetilde{\Phi}_{\mathrm{S}} + \widehat{\Phi}_{\mathrm{D}}$ as total tension and angle of the system, respectively.
Dynamic equilibrium in $\underline{t}$ and $\underline{n}$ directions are given by:

$$\underline{t} \quad \begin{cases} \dfrac{\mathrm{d}\widetilde{T}_{\mathrm{S}}}{\mathrm{d}s} + \dfrac{\partial \widehat{T}_{\mathrm{D}}}{\partial s} - w(\sin(\widetilde{\Phi}_{\mathrm{S}}) + \widehat{\Phi}_{\mathrm{D}} \cos(\widetilde{\Phi}_{\mathrm{S}})) \\ \qquad\qquad = \dfrac{\mathrm{D}}{\mathrm{D}t} \left\{ m \left(\mathrm{V}\, \underline{t} + \hat{p}\, \underline{t} + \hat{q}\, \underline{n} \right) \right\} \cdot\ \underline{t} \end{cases} \tag{6}$$

$$\underline{n} \quad \begin{cases} (\widetilde{T}_{\mathrm{S}} + \widehat{T}_{\mathrm{D}}) \dfrac{\mathrm{d}\widetilde{\Phi}_{\mathrm{S}}}{\mathrm{d}s} + \widetilde{T}_{\mathrm{S}} \dfrac{\partial \widehat{\Phi}_{\mathrm{D}}}{\partial s} - w(\cos(\widetilde{\Phi}_{\mathrm{S}}) - \widehat{\Phi}_{\mathrm{D}} \sin \widetilde{\Phi}_{\mathrm{S}}) \\ \qquad\qquad = \dfrac{\mathrm{D}}{\mathrm{D}t} \left\{ m \left(\mathrm{V}\, \underline{t} + \hat{p}\, \underline{t} + \hat{q}\, \underline{n} \right) \right\} \cdot\ \underline{n} \end{cases} \tag{7}$$

Let us express conditions for the dynamic tension $\widehat{T}_{\mathrm{D}}$ and dynamic angle $\widehat{\Phi}_{\mathrm{D}}$ to be compatible with the dynamic displacements $\hat{p}$ and $\hat{q}$. The latter can be obtained via imposing geometrical conditions, which are depicted in Fig.(1). Following compatibility conditions is set [11]:

$$e_{\mathrm{d}} = \frac{\partial \hat{p}}{\partial s} - \hat{q} \frac{\mathrm{d}\widetilde{\Phi}_{\mathrm{S}}}{\mathrm{d}s} \tag{8}$$

$$\widehat{\Phi}_{\mathrm{D}} = \hat{p} \frac{\mathrm{d}\widetilde{\Phi}_{\mathrm{S}}}{\mathrm{d}s} + \frac{\partial \hat{q}}{\partial s} \tag{9}$$

Where e_{d} is the dynamic strain of the cable which can be linked to the dynamic tension via the Hooke's law as $e_{\mathrm{d}} = \frac{\widehat{T}_{\mathrm{D}}}{EA}$. In the next section, after providing some simplifying assumptions, the dynamics equations will be derived.

2.3 Governing equations of the system

Let us suppose that:

$$\begin{cases} \widehat{\Phi}_{\mathrm{D}} \ll 1 \\ \dfrac{\mathrm{d}\widetilde{\Phi}_{\mathrm{S}} + \mathrm{d}\widehat{\Phi}_{\mathrm{D}}}{2} \ll 1 \\ \widehat{T}_{\mathrm{D}} \dfrac{\mathrm{d}\widehat{\Phi}_{\mathrm{D}}}{2} \ll 1 \end{cases} \tag{10}$$

Expansion at first order of $\sin$ and $\cos$ are done as:

$$\begin{cases} \sin(\widetilde{\Phi}_{\mathrm{S}} + \widehat{\Phi}_{\mathrm{D}}) \approx \sin(\widetilde{\Phi}_{\mathrm{S}}) + \widehat{\Phi}_{\mathrm{D}} \cos(\widetilde{\Phi}_{\mathrm{S}}) \\ \cos(\widetilde{\Phi}_{\mathrm{S}} + \widehat{\Phi}_{\mathrm{D}}) \approx \cos(\widetilde{\Phi}_{\mathrm{S}}) - \widehat{\Phi}_{\mathrm{D}} \sin(\widetilde{\Phi}_{\mathrm{S}}) \end{cases} \tag{11}$$

Then equations of the reference configuration (see Eqs.(2) and (3)) and the dynamic angle compatibility condition (Eq.(9)) are injected to Eqs.(6) and (7). Following system is obtained:

$$\underline{t}\ :\quad \begin{bmatrix} m\dfrac{\partial^2\hat{p}}{\partial t^2}+m\mathrm{V}^2\left[\dfrac{\partial^2\hat{p}}{\partial s^2}-3\dfrac{\mathrm{d}\widetilde{\Phi}_{\mathrm{S}}}{\mathrm{d}s}\dfrac{\partial\hat{q}}{\partial s}-\dfrac{\mathrm{d}^2\widetilde{\Phi}_{\mathrm{S}}}{\mathrm{d}s^2}\hat{q}-2\left(\dfrac{\mathrm{d}\widetilde{\Phi}_{\mathrm{S}}}{\mathrm{d}s}\right)^2\hat{p}\right] \\ -2m\mathrm{V}\left[\dfrac{\mathrm{d}\widetilde{\Phi}_{\mathrm{S}}}{\mathrm{d}s}\dfrac{\partial\hat{q}}{\partial t}-\dfrac{\partial^2\hat{p}}{\partial t\partial s}\right]=\dfrac{\partial\widehat{T}_{\mathrm{D}}}{\partial s}-\widetilde{T}_{\mathrm{S}}\dfrac{\mathrm{d}\widetilde{\Phi}_{\mathrm{S}}}{\mathrm{d}s}\left[\dfrac{\partial\hat{q}}{\partial s}+\dfrac{\mathrm{d}\widetilde{\Phi}_{\mathrm{S}}}{\mathrm{d}s}\hat{p}\right] \end{bmatrix} \tag{12}$$

$$\underline{n}\ :\quad \begin{bmatrix} m\dfrac{\partial^2\hat{q}}{\partial t^2}+m\mathrm{V}^2\left[\dfrac{\partial^2\hat{q}}{\partial s^2}+2\dfrac{\mathrm{d}\widetilde{\Phi}_{\mathrm{S}}}{\mathrm{d}s}\dfrac{\partial\hat{p}}{\partial s}+\dfrac{\mathrm{d}^2\widetilde{\Phi}_{\mathrm{S}}}{\mathrm{d}s^2}\hat{p}-\left(\dfrac{\mathrm{d}\widetilde{\Phi}_{\mathrm{S}}}{\mathrm{d}s}\right)^2\hat{q}\right] \\ +2m\mathrm{V}\left[\dfrac{\mathrm{d}\widetilde{\Phi}_{\mathrm{S}}}{\mathrm{d}s}\dfrac{\partial\hat{p}}{\partial t}+\dfrac{\partial^2\hat{q}}{\partial t\partial s}\right]=\hat{p}\left(\dfrac{\mathrm{d}^2\widetilde{\Phi}_{\mathrm{S}}}{\mathrm{d}s^2}\widetilde{T}_{\mathrm{S}}+\dfrac{\mathrm{d}\widetilde{T}_{\mathrm{S}}}{\mathrm{d}s}\dfrac{\mathrm{d}\widetilde{\Phi}_{\mathrm{S}}}{\mathrm{d}s}\right) \\ +\widetilde{T}_{\mathrm{S}}\left[\dfrac{\partial^2\hat{q}}{\partial s^2}+\dfrac{\mathrm{d}\widetilde{\Phi}_{\mathrm{S}}}{\mathrm{d}s}\dfrac{\partial\hat{p}}{\partial s}\right]+\widehat{T}_{\mathrm{D}}\dfrac{\mathrm{d}\widetilde{\Phi}_{\mathrm{S}}}{\mathrm{d}s}+\dfrac{\mathrm{d}\widetilde{T}_{\mathrm{S}}}{\mathrm{d}s}\dfrac{\partial\hat{q}}{\partial s} \end{bmatrix} \tag{13}$$

Spatio temporal variables of Eqs.(12 and 13) can be separated as:

$$\begin{bmatrix} \hat{q}(s,t)=q(s)e^{i\omega t} \\ \hat{p}(s,t)=p(s)e^{i\omega t} \\ \widehat{T}_{\mathrm{D}}(s,t)=T_D(s)e^{i\omega t} \end{bmatrix} \tag{14}$$

where $i^2=-1$.
We will treat the problem with space variables via the SMSM [18] which is explained in the next section.

3 The space multiple scale method

In this section, a SMSM is exploited in which the small coupling parameter between different scales of space has a physical sense, i.e. it is not a book-keeping parameter. Then, the static equilibrium has been expanded versus this small parameter. Moreover, we suppose that the dynamic behavior of the system is carried out around the static equilibrium. Finally, for detecting the system responses, different orders of system equations and compatibility conditions with respect to the small coupling parameter are distinguished.
Let us treat Eqs.(12) and (13) with the SMSM [18]. To this end, we introduce a small dimensionless parameter $0<\epsilon\ll 1$, which is used to introduce different space variables couples to each other via ϵ parameter:

$$s_0=s \tag{15}$$

$$s_k=\epsilon^k s_0 \quad ; \quad \forall k\in\mathbb{N}^* \tag{16}$$

We use the notation D_k to refer to the operator $\frac{\partial}{\partial s_k}$. So, [18]

$$\frac{\partial}{\partial s}=D_0+\epsilon D_1+\epsilon^2 D_2+... \tag{17}$$

$$\frac{\partial^2}{\partial s^2}=D_0^2+2\epsilon D_0D_1+\epsilon^2\left(D_1^2+2D_0D_2\right)+... \tag{18}$$

The coupling parameter of the SMSM, i.e. ϵ parameter, reads:

$$\frac{1}{\widetilde{T}_a}\int_0^L w\mathrm{d}s=\frac{wL}{\widetilde{T}_a}=\epsilon \tag{19}$$

This parameter is in fact the ratio of the cable self-weight and the reference tension. In the limit case when $\epsilon \to 0$, the system tends to governing equation of a rope model.
We expand the static tension and angle as:

$$\widetilde{T}_{\mathrm{S}} = \widetilde{T}_a \left[1 + \epsilon \sin\widetilde{\Phi}_a \frac{s-s_a}{L} + \epsilon^2 \frac{\widetilde{T}_a (\cos\widetilde{\Phi}_a)^2}{2(\widetilde{T}_a - m\mathrm{V}^2)} \left(\frac{s-s_a}{L} \right)^2 \right] + \mathcal{O}(\epsilon^3) \tag{20}$$

$$\frac{\mathrm{d}\widetilde{\Phi}_{\mathrm{S}}}{\mathrm{d}s} = \frac{\epsilon}{L} \frac{\widetilde{T}_a \cos\widetilde{\Phi}_a}{\widetilde{T}_a - m\mathrm{V}^2} \left[1 - 2\epsilon \frac{\widetilde{T}_a \sin\widetilde{\Phi}_a}{\widetilde{T}_a - m\mathrm{V}^2} \frac{s-s_a}{L} \right] + \mathcal{O}(\epsilon^2) \tag{21}$$

and we set:

$$\widetilde{T}_{\mathrm{S}} = \widetilde{T}_a + \sum_{k=1}^{N} \epsilon^k \widetilde{\xi}_k(s_0) \tag{22}$$

$$\frac{\mathrm{d}\widetilde{\Phi}_{\mathrm{S}}}{\mathrm{d}s} = \epsilon\widetilde{\chi}_1 + \sum_{k=2}^{N} \epsilon^k \widetilde{\chi}_k(s_0) \tag{23}$$

Where $\widetilde{\xi}_k$ and $\widetilde{\chi}_k$ are the associated coefficient of the monomial $(s-s_a)^k$ in the expansion of static tension and angle respectively.
To treat system equations via a SMSM, we expand system variables as:

$$\begin{aligned} q(s) =& \epsilon q_1(s_0, s_2, s_2, ...) + \epsilon^2 q_2(s_0, s_2, s_2, ...) + ... \\ p(s) =& \epsilon^2 p_2(s_0, s_2, s_2, ...) + \epsilon^3 p_3(s_0, s_2, s_2, ...) + ... \\ T_D(s) =& \widetilde{T}_a \left[\epsilon T_1(s_0, s_2, s_2, ...) + \epsilon^2 T_2(s_0, s_2, s_2, ...) + ... \right] \end{aligned} \tag{24}$$

where $\widetilde{T}_a T_1$ and $\widetilde{T}_a T_2$ are the first and the second order terms of the expansion of the dynamic tension increment. It follows that, T_1 and T_2 are non dimensional terms.

3.1 Multiple scale analysis of the system

Let us substitute expanded system variables defined in Eq.(24) in system Eqs.(12) and (13). The following equations can be obtained at first and second orders of ϵ:

$$\mathcal{O}\left(\epsilon^1\right): \quad \begin{cases} \left(\widetilde{T}_a - m\mathrm{V}^2\right) D_0^2 q_1 - 2im\mathrm{V}\omega D_0 q_1 + m\omega^2 q_1 = 0 \\ \widetilde{T}_a D_0 T_1 = 0 \end{cases} \tag{25}$$

$$\mathcal{O}\left(\epsilon^2\right): \quad \begin{cases} \left(\widetilde{T}_a - m\mathrm{V}^2\right) D_0^2 q_2 - 2im\mathrm{V}\omega D_0 q_2 + m\omega^2 q_2 = -\widetilde{T}_a \widetilde{\chi}_1 T_1 \\ \qquad - 2\left(\widetilde{T}_a - m\mathrm{V}^2\right) D_1 D_0 q_1 + 2im\mathrm{V}\omega D_1 q_1 \\ \qquad - \widetilde{\xi}_1 D_0^2 q_1 - D_0 q_1 D_0 \widetilde{\xi}_1 \\ \\ - m\mathrm{V}^2 D_0^2 p_2 - 2im\mathrm{V}\omega D_0 p_2 + m\omega^2 p_2 = -\widetilde{T}_a \left(D_1 T_1 + D_0 T_2\right) \\ \qquad + \widetilde{\chi}_1 \left[\left(\widetilde{T}_a - 3m\mathrm{V}^2\right) D_0 q_1 - 2im\mathrm{V}\omega q_1 \right] \end{cases} \tag{26}$$

These equations provide insight about the behavior of the system at the space scales s_0 and s_1. We clearly see that the velocity induces complex behavior for the system at $\mathcal{O}\left(\epsilon^1\right)$. Moreover, the normal displacement q_1 is acting as source of excitation for q_2. The pure velocity dependant terms coming with $D_0 q_1$, $D_0 q_2$ and $D_0 p_2$ in Eqs.(25) and (26) creates waves that are propagating with different velocities. Moreover, the dynamic tension is spotted to be

independent of the first space scale s_0, that is consistent with our assumptions of small perturbation of the static equilibrium.
Equation (24) can be substituted into Eq.(8) which provides some relationships between axial and normal displacements as:

$$e_{\mathrm{d}} = \frac{\widehat{T}_{\mathrm{D}}}{EA} = \frac{\partial \hat{p}}{\partial s} - \hat{q}\frac{\mathrm{d}\widetilde{\Phi}_{\mathrm{S}}}{\mathrm{d}s} \rightarrow \begin{cases} \mathcal{O}(\epsilon^2) \;\; 0 = D_0 p_2 - q_1 \widetilde{\chi}_1 \\ \mathcal{O}(\epsilon^3) \;\; \alpha T_1 = D_0 p_3 + D_1 p_2 - q_1 \widetilde{\chi}_2 - q_2 \widetilde{\chi}_1 \end{cases} \tag{27}$$

Where we assume that:

$$\frac{\widetilde{T}_a}{EA} = \epsilon^2 \alpha \tag{28}$$

The next step will be to evaluate modal characteristics of the system which are provided in section (4).

4 Frequencies and modes of the translating cable

In this section, the equations obtained from the SMSM are treated with two different methodologies. First, an analytical approach (see section 4.1) is used to provide a family of solutions for q_1. Then, a analytic-numerical technique based on expansion of system variables with the Fourier series (see section 4.2) is endowed to get frequencies and modes for the system. Finally, a fully numerical approach based on finite difference method (FDM) is presented in section 4.3 to detect the modal characteristics of the system.

4.1 Analytical approach

Here, we are seeking for q_1 as a function of s_0 and $s_1$via exploiting the SMSM in its classical manner.
From the first set of equations (25) we can write:

$$q_1(s_0, s_1) = A(s_1)e^{i\omega a s_0} + B(s_1)e^{i\omega b s_0} \tag{29}$$

with:

$$\begin{cases} a = \dfrac{m\mathrm{V} + \sqrt{m\widetilde{T}_a}}{\widetilde{T}_a - m\mathrm{V}^2} \\ b = \dfrac{m\mathrm{V} - \sqrt{m\widetilde{T}_a}}{\widetilde{T}_a - m\mathrm{V}^2} \end{cases} \tag{30}$$

By injection of Eq.(29) in Eq.(26), we obtain the following system:

$$\begin{aligned} \left(\widetilde{T}_a - m\mathrm{V}^2\right) D_0^2 q_2 - 2im\mathrm{V}\omega D_0 q_2 + m\omega^2 q_2 = & -\widetilde{T}_a \widetilde{\chi}_1 T_1 \\ & + a\omega \left(\xi A(s_1)(as_0\omega - i) - 2i\widetilde{T}_a D_1 A(s_1)\right) e^{ias_0\omega} \\ & + b\omega \left(\xi B(s_1)(bs_0\omega - i) - 2i\widetilde{T}_a D_1 B(s_1)\right) e^{ibs_0\omega} \end{aligned} \tag{31}$$

It can be seen that q_2 diverges due to secular terms. If not removed, these terms prevent to find modes and frequencies unless the velocity satisfies $\mathrm{V} = 0$ which is not relevant for our study.
Solvability conditions are then applied to get information about the modes of the system. As T_1 is not a function of s_0, A_1 and B_1 must satisfy:

$$\xi A(s_1)(as_0\omega - i) - 2i\widetilde{T}_a D_1 A(s_1) = 0 \tag{32}$$

$$\xi B(s_1)(bs_0\omega - i) - 2i\widetilde{T}_a D_1 B(s_1) = 0 \tag{33}$$

As A and B are functions of s_1 only, as_0 and bs_0 have to be rescaled to s_1. That is to say:

$$\xi A(s_1)(\tilde{a}s_1\omega - i) - 2i\widetilde{T}_a D_1 A(s_1) = 0 \tag{34}$$

$$\xi B(s_1)(\tilde{b}s_1\omega - i) - 2i\widetilde{T}_a D_1 B(s_1) = 0 \tag{35}$$

where $\tilde{a} = \dfrac{\mathrm{V} + \sqrt{\frac{\widetilde{T}_a}{m}}}{gL\left(1 - \frac{m\mathrm{V}^2}{\widetilde{T}_a}\right)}$ and $\tilde{b} = \dfrac{\mathrm{V} - \sqrt{\frac{\widetilde{T}_a}{m}}}{gL\left(1 - \frac{m\mathrm{V}^2}{\widetilde{T}_a}\right)}$.

From Eqs.(34) and (35), we obtain:

$$A(s_1) = A_1 e^{-\frac{\xi s_1}{2\widetilde{T}_a}} \left(\cos\left(\frac{\tilde{a}\xi s_1^2 \omega}{4\widetilde{T}_a}\right) - i \sin\left(\frac{\tilde{a}\xi s_1^2 \omega}{4\widetilde{T}_a}\right)\right) \tag{36}$$

$$B(s_1) = B_1 e^{-\frac{\xi s_1}{2\widetilde{T}_a}} \left(\cos\left(\frac{\tilde{b}\xi s_1^2 \omega}{4\widetilde{T}_a}\right) - i \sin\left(\frac{\tilde{b}\xi s_1^2 \omega}{4\widetilde{T}_a}\right)\right) \tag{37}$$

and via considering boundary conditions $q(0) = q(L) = 0$, we have:

$$q_1(0,0) = 0 \leftrightarrow B_1 = -A_1 \tag{38}$$

Then:

$$q_1(L, \epsilon L) = A_1 e^{-\frac{L\xi\epsilon}{2\widetilde{T}_a}} \left(e^{-\frac{iL\omega\left(\tilde{a}L\xi\epsilon^2 - 4a\widetilde{T}_a\right)}{4\widetilde{T}_a}} - e^{-\frac{iL\omega\left(\tilde{b}L\xi\epsilon^2 - 4b\widetilde{T}_a\right)}{4\widetilde{T}_a}} \right) \tag{39}$$

$$q_1(L, \epsilon L) = 0 \leftrightarrow \omega = \frac{8\pi k \widetilde{T}_a}{4(a-b)L\widetilde{T}_a - \xi(\epsilon L)^2(\tilde{a} - \tilde{b})} \quad ; \quad k \in \mathrm{Z} \tag{40}$$

We find a family of solution denoted as $(q_{1,k})_{k\in\mathbb{N}}$:

$$q_{1,k}(s_0, s_1) = \frac{1}{2} e^{\left[-\frac{\xi s_1}{2\widetilde{T}_a}\right]} \left(e^{\left[-\frac{2i\pi k\left(4as_0\widetilde{T}_a - \tilde{a}\xi s_1^2\right)}{L\left(4\widetilde{T}_a(a-b) - L\xi\epsilon^2(\tilde{a}-\tilde{b})\right)}\right]} - e^{\left[-\frac{2i\pi k\left(4bs_0\widetilde{T}_a - \tilde{b}\xi s_1^2\right)}{L\left(4\widetilde{T}_a(a-b) - L\xi\epsilon^2(\tilde{a}-\tilde{b})\right)}\right]} \right) \tag{41}$$

It can be shown that these solutions have nodes ($\mathcal{N}$) and local maximum ($\mathcal{V}$):

$$\mathcal{N}(n,k) = \frac{L\left(4(a-b)\widetilde{T}_a - L\xi\epsilon^2(\tilde{a}-\tilde{b})\right)}{\sqrt{\mathcal{Z}} + 2k\widetilde{T}_a(a-b)} n \tag{42}$$

where $n \in [0, k]$ and:

$$\mathcal{Z} = k\left(-4Ln\xi\widetilde{T}_a\epsilon^2(a-b)(\tilde{a}-\tilde{b}) + 4k\widetilde{T}_a^2(a-b)^2 + L^2 n\xi^2\epsilon^4(\tilde{a}-\tilde{b})^2\right) \tag{43}$$

$$\mathcal{V}(n,k) = \frac{\sqrt{2\mathcal{X}}L\left(4\widetilde{T}_a(b-a) + L\xi\epsilon^2(\tilde{a}-\tilde{b})\right)}{2k\xi\epsilon^2(\tilde{a}-\tilde{b})} + \frac{2\widetilde{T}_a(b-a)}{\xi\epsilon^2(\tilde{b}-\tilde{a})} \tag{44}$$

where $n \in [1, k]$ and:

$$\begin{aligned}\mathcal{X} = &\frac{8k\widetilde{T}_a^2(a-b)^2 - 4L(2n-1)\xi\widetilde{T}_a\epsilon^2(a-b)(\tilde{a}-\tilde{b})}{L^2\left(4\widetilde{T}_a(b-a) + L\xi\epsilon^2(\tilde{a}-\tilde{b})\right)^2} k \\ &+ \frac{(2n-1)\xi^2\epsilon^4(\tilde{a}-\tilde{b})^2}{\left(4\widetilde{T}_a(b-a) + L\xi\epsilon^2(\tilde{a}-\tilde{b})\right)^2} k\end{aligned} \tag{45}$$

4.1.1 An example

Parameters used for the translating catenary are displayed in Tab.(1). The reference abscissa used in further calculation is $s_a = 0$, then the initial point of the span corresponds to initial tension $\widetilde{T}_{\mathrm{S}}(0)$. The modes 1 to 5 are plotted with their corresponding frequency for two different translation veolicities: $\mathrm{V} = 0$ and $\mathrm{V} = 7.5$ m.s^{-1}. The current approach allows to exhibit modes for a translating catenary believed to be asymptotically valid for the fixed end cable as the analytic expression of A and B satisfying that $B = A^*$ when $\mathrm{V} = 0$. The superscript $(\cdot)^*$ stands for the complex conjugate of the variable. When $\mathrm{V} \neq 0$, the modes become complex. The amplitude of the real and imaginary part contribute to provide a purely decreasing (respectively increasing) amplitude. Those can be seen on the Fig.(2). We obtain that:

$\widetilde{T}_a$ (N)	$\widetilde{\Phi}_a$ ($^\circ$)	m (kg.m^{-1})	g (m.s^{-2})	w (kg.s^{-2})	L (m)
86600	23.43	5.56	9.81	mg	330

Table 1: Parameters of the system under consideration. This table is used in the whole paper for numerical examples

- The frequency of the mode is a decreasing function of V^2.
- Translation catenary exhibit complex mode behavior with an unbalanced amplitude between the real and imaginary parts.

4.2 Seeking system modes via analytic-numerical approximation

In the following developments, a method to derive numerical solution to the governing equations is detailed based on the use of Fourier series expansion.
Equation (25) provides:

$$D_0 T_1 = 0 \leftrightarrow T_1 = T_1(s_1, ...) \tag{46}$$

Let us apply D_0 to the second equation of the set Eq.(26):

$$\begin{aligned} -m\mathrm{V}^2 D_0^3 p_2 - 2im\mathrm{V}\omega D_0^2 p_2 + m\omega^2 D_0 p_2 = -\widetilde{T}_a \left(D_1 D_0 T_1 + D_0^2 T_2\right) \\ + \widetilde{\chi}_1 \left[\left(\widetilde{T}_a - 3m\mathrm{V}^2\right) D_0^2 q_1 - 2im\mathrm{V}\omega D_0 q_1\right] \end{aligned} \tag{47}$$

It has been already demonstrated that T_1 is independent of s_0. In this study we assume that T_2 is independent from s_0 as well. Substituting Eq.(27) into Eq.(47), we obtain:

$$\begin{aligned} -m\mathrm{V}^2 D_0^2(\widetilde{\chi}_1 q_1) - 2im\mathrm{V}\omega D_0(\widetilde{\chi}_1 q_1) + m\omega^2(\widetilde{\chi}_1 q_1) \\ = \widetilde{\chi}_1 \left[\left(\widetilde{T}_a - 3m\mathrm{V}^2\right) D_0^2 q_1 - 2im\mathrm{V}\omega D_0 q_1\right] \end{aligned} \tag{48}$$

If we inject Eq.(29) in Eq.(48), the following can be obtained:

$$B(s_1, s_2, ...) = -\frac{a^2\left(\widetilde{T}_a - 2m\mathrm{V}^2\right) + m}{b^2\left(\widetilde{T}_a - 2m\mathrm{V}^2\right) + m} A(s_1, s_2, ...) e^{[i(a-b)\omega s_0]} \tag{49}$$

$$= -\gamma A(s_1, s_2, ...) e^{[i(a-b)\omega s_0]} \tag{50}$$

As B is a function of s_1 only, this equation is re-scaled via:

$$a - b = 2\epsilon\frac{\nu}{\mathrm{V}} \tag{51}$$

with:

$$\nu = \frac{\mathrm{V}\sqrt{m\widetilde{T}_a}}{\widetilde{T}_a - m\mathrm{V}^2} \tag{52}$$

Then:

$$q_1 = A(s_1, ...)\left[e^{(i\omega a s_0)} - \gamma e^{i\Omega s_1} e^{(i\omega b s_0)}\right] \tag{53}$$

with:

$$\Omega = 2\omega\frac{\nu}{\mathrm{V}} \tag{54}$$

Eq.(26) can be read as:

$$\mathcal{L}(q_2) = \mathcal{F}(s_0, s_1) \tag{55}$$

Where $\mathcal{L}$ is the operator applied on q_2 and $\mathcal{F}(s_0, s_1)$ is the right hand side of the differential equation.
To ensure solvability condition for q_2 and to get information about $A(s_1)$, we apply the Fredholm alternative [19]

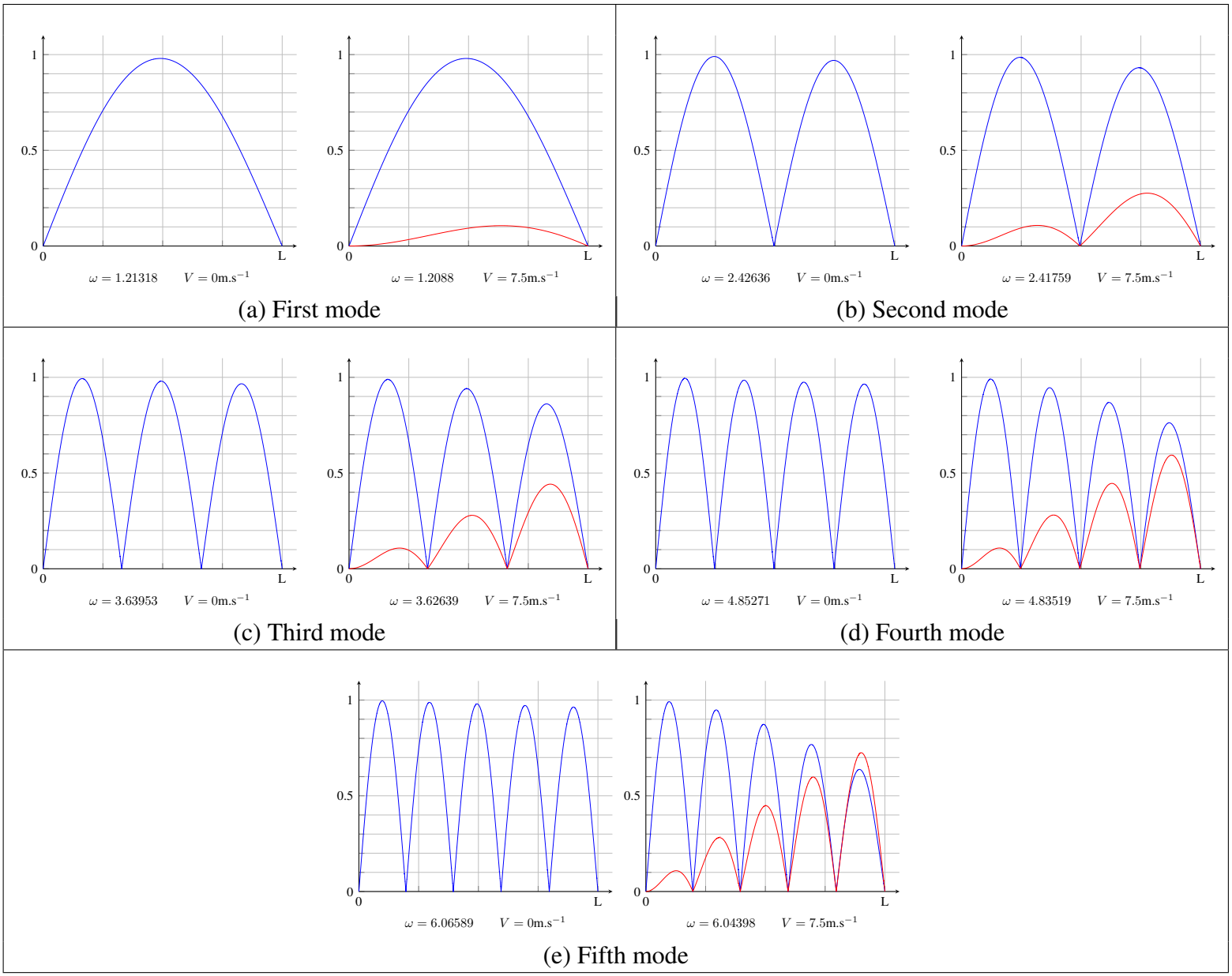

Figure 2: Absolute value of the real (—) and the imaginary (—) parts of the first five modes obtained from Eq.(41); ω is computed from to Eq.(40)

to the system under consideration. It can be easily proven that $\mathcal{L}$ is self adjoint for the canonical inner product of $\mathcal{C}^2([0,L],\mathrm{C})$ when the cable hangs between ideal supports (i.e. $q(0)=q(L)=0$). Solvability conditions are then obtained by satisfying [19]:

$$\int_0^L \mathcal{F}(s_0,s_1)\ P^*\ \mathrm{d}s_0 = 0 \tag{56}$$

where P is a variable of the kernel of $\mathcal{L}$:

$$P(s_0,s_1) = P_1(s_1,...)e^{i\omega a s_0} + P_2(s_1,...)e^{i\omega b s_0} \tag{57}$$

This kernel is of finite dimension, as needed for Fredholm Alternative [19].
Two equations can be obtained, which shapes are:

$$\alpha_1 A(s_1) + \alpha_2 D_1 A(s_1) + i\frac{\widetilde{\chi}_1\widetilde{T}_a T_1\left(1-e^{-iaL\omega}\right)}{a\omega} = 0 \tag{58}$$

$$\alpha_3 A(s_1) + \alpha_4 D_1 A(s_1) + i\frac{\widetilde{\chi}_1\widetilde{T}_a T_1\left(1-e^{-ibL\omega}\right)}{b\omega} = 0 \tag{59}$$

The α_i coefficients are provided in A.
Thanks to Eqs.(58) and (59), the variable T_1 can be dropped. Following differential equation in A is obtained:

$$\forall s_1 \in [0,L], \quad \left(\Sigma + \Gamma e^{i\Omega_1 s_1}\right) D_1 A + \left(\Pi + \Delta e^{i\Omega_1 s_1}\right) A = 0 \tag{60}$$

Variables Σ, Γ, Π and Δ are presented in B.

4.2.1 Frequencies and mode shapes approximation by using truncated Fourier series

We seek for a solution of A as:

$$A(s_1) = \sum_{n=-\infty}^{n=+\infty} a_n e^{-in\Omega_1 s_1} \quad \forall n \in \mathrm{Z}, a_n \in \mathrm{C} \tag{61}$$

After substitution of this infered solution into Eq.(60) and truncation at N, the following holds:

$$\sum_{n=-N}^{N}\left[\left(\Pi + \frac{\Omega_1\Sigma}{i}n\right)a_n + \left(\Delta + \frac{\Omega_1\Gamma}{i}(n+1)\right)a_{n+1}\right]e^{-in\Omega_1 s_1} = 0 \tag{62}$$

i.e.,

$$\sum_{n=-N}^{N}\left[\Pi_n a_n + \Delta_{n+1}a_{n+1}\right]e^{-in\Omega_1 s_1} = 0 \tag{63}$$

$2N+1$ equations are obtained through this process which shall be supplemented by two boundary condition yielding to:

$$\begin{cases} \displaystyle\sum_{n=-N}^{N} a_n = 0 \\ \displaystyle\sum_{n=-N}^{N} a_n e^{-i\Omega_1 L} = 0 \end{cases} \tag{64}$$

The full set of equations in the matrix form reads:

$$\mathbf{M}_N \begin{bmatrix} a_{-N} \\ \vdots \\ a_N \end{bmatrix} = \begin{bmatrix} 0 \\ \vdots \\ 0 \end{bmatrix} \quad \text{where} \quad \mathbf{M}_N = \begin{bmatrix} 1 & \dots & 1 & 1 \\ \Pi_{-N} & \Delta_{1-N} & 0 & \\ 0 & \ddots & \ddots & \\ \vdots & \ddots & \Pi_{N-1} & \Delta_N \\ 0 & \dots & 0 & \Pi_N \\ e^{iN\Omega_1 L} & \dots & e^{-i(N-1)\Omega_1 L} & e^{-iN\Omega_1 L} \end{bmatrix}_{(2N+3,2N+1)} \tag{65}$$

N	ω_1	ω_2	ω_3	ω_4	ω_5
1	/	2.38	/	4.75	5.72
2	/	2.38	/	4.75	5.72
3	/	2.38	/	4.75	5.72
4	/	2.38	/	4.75	5.72
5	/	2.38	/	4.75	5.72
10	/	2.38	/	4.75	5.72
15	/	2.38	/	4.75	5.72
20	/	2.38	/	4.75	5.72 / 5.94
22	1.10	2.38/2.68	/	4.59/4.91	5.72 / 5.94
25	1.10	2.38 / 2.411	3.25	4.75	5.72
50	/	2.38	/	4.75	5.72

Table 2: Obtained solutions based on truncated Fourier series with error tolerance of 10^{-12} as a function of N for the system with V $= 0$; Symbol / stands for a non traced mode

In order to seek for admissible ω to obtain periodic motion, the $\mathbf{M}_N$ matrix should be square. A truncation method appears to be the more praticable solution for this purpose. In order to keep as much information as possible, we drop the 2$^{\text{nd}}$ and $2N + 2^{\text{th}}$ rows of the matrix. The problem reads:

$$\mathbf{T}_N \begin{bmatrix} a_{-N} \\ \vdots \\ a_N \end{bmatrix} = \begin{bmatrix} 0 \\ \vdots \\ 0 \end{bmatrix} \quad \text{where} \quad \mathbf{T}_N = \begin{bmatrix} 1 & 1 & \dots & 1 & 1 \\ 0 & \Pi_{1-N} & \Delta_{2-N} & 0 & \dots \\ \vdots & \ddots & \ddots & \ddots & \ddots \\ 0 & \dots & 0 & \Pi_{N-1} & \Delta_N \\ e^{iN\Omega_1 L} & & \dots & & e^{-iN\Omega_1 L} \end{bmatrix}_{(2N+1,2N+1)} \tag{66}$$

We can now seek for the admissible ω which satisfy $\det(\mathbf{T}_N) = 0$. Then we can have the modes of the system by solving the matrix system, i.e. we find non trivial $(a_n)_{n\in[-N,N]}$ which generate a family of solutions for a given ω.

4.2.2 An example:

Let us suppose V $= 0$ in order to compare the obtained results with the ones obtained earlier by Irvine [1] and Tryantafyllou [20]. The results are obtained via evaluation of roots of $\det(\mathbf{T}_N)$ in Mathematica® (see Eq.(66)). Obtained frequencies based on different N parameter of the Fourier series (see Eq.(61)) are collected in Tab.(2). When N increases, the precision of some of the obtained roots augment via consideration of more significant figures. However, some frequencies are really difficult to trace numerically without decreasing the accuracy criterion (for instance the ones corresponding to modes 1 and 3). Thanks to this approach we found some frequencies close to those detected by Irvine in [1] (and also Triantafyllou [20]) for a fixed cable but other frequencies corresponding to the first and fifth modes are slightly different. Modes 6 to 9 are found during calculations respectively corresponding to $\omega = 7.12867$, $\omega = 9.5049$, $\omega = 11.874$ and $\omega = 14.2574$.
Mode shapes can be obtained via a_n coefficients Eq.(65). To give insight about the envelope of these modes, figures are provided with small value of N. Even if more harmonics provides more precision in calculation of the frequency (as seen in Figs.(3) and (4)), the stiffness of the numerical problem in evaluating frequencies is a big limitation for further calculations. However, independently of the number of harmonics, the nodes and local extrema are well localized regardless of parameter N. Moreover, comparisons with earlier developments are easier with results obtained based on the single harmonic assumption. To plot modes with small number of N and to get smooth curves, tolerances of error have been reduced to obtain modes 1 and 3. Obtained curves are displayed in Fig.(5). Those modes are normalized with respect to their maximum values, so that each figure reaches 1 at its maximum. The figures show that the number of local maxima and nodes are not consistent with classical results obtained with a fixed cable [1]. This is a limitation to this methodology, at least for the case when V $= 0$. Mode shapes are not symmetric or even antisymmetric and the number of nodes is not following the increase of the frequency as

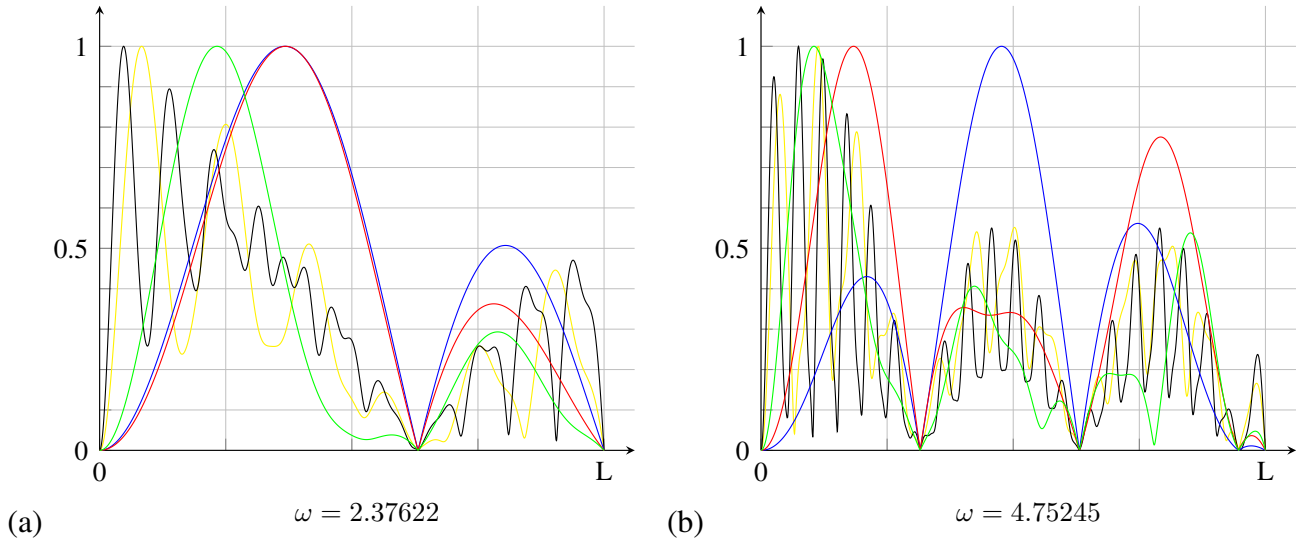

Figure 3: Mode shapes of the cable: (a) mode 2; (b) mode 4. These modes are obtained based on considering $N = 1$ (—) , $N = 2$ (—) , $N = 5$ (—) , $N = 15$ (—) and $N = 25$ (—) in Eq.(66)

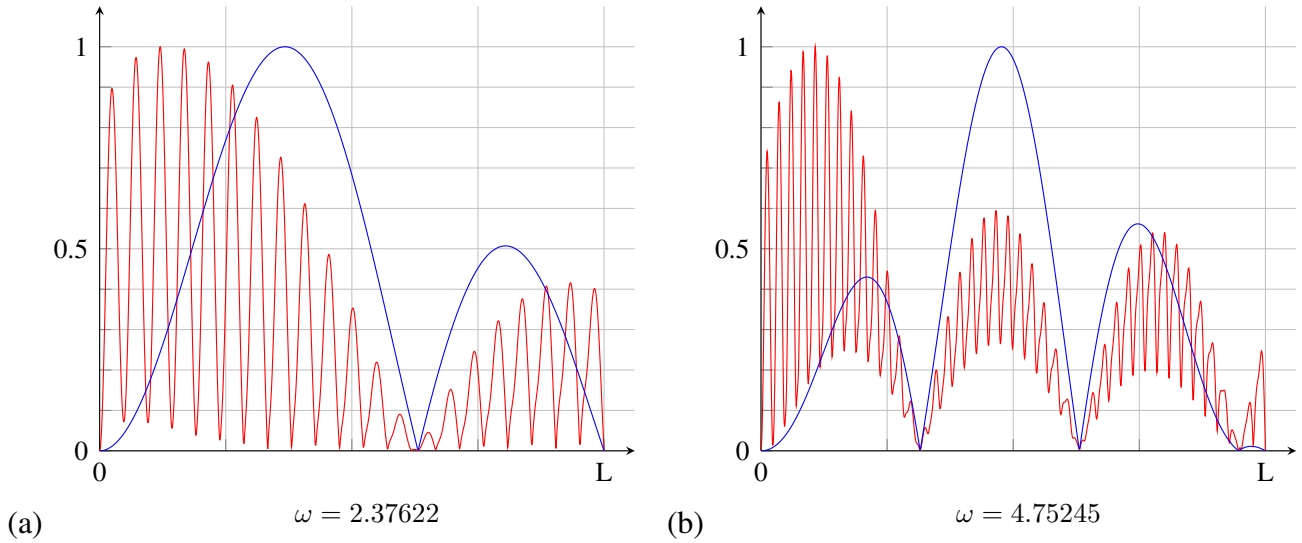

Figure 4: Mode shapes of the cable: (a) mode 2; (b) mode 4. These modes are obtained based on considering $N = 1$ (—) and $N = 50$ (—) in Eq.(66)

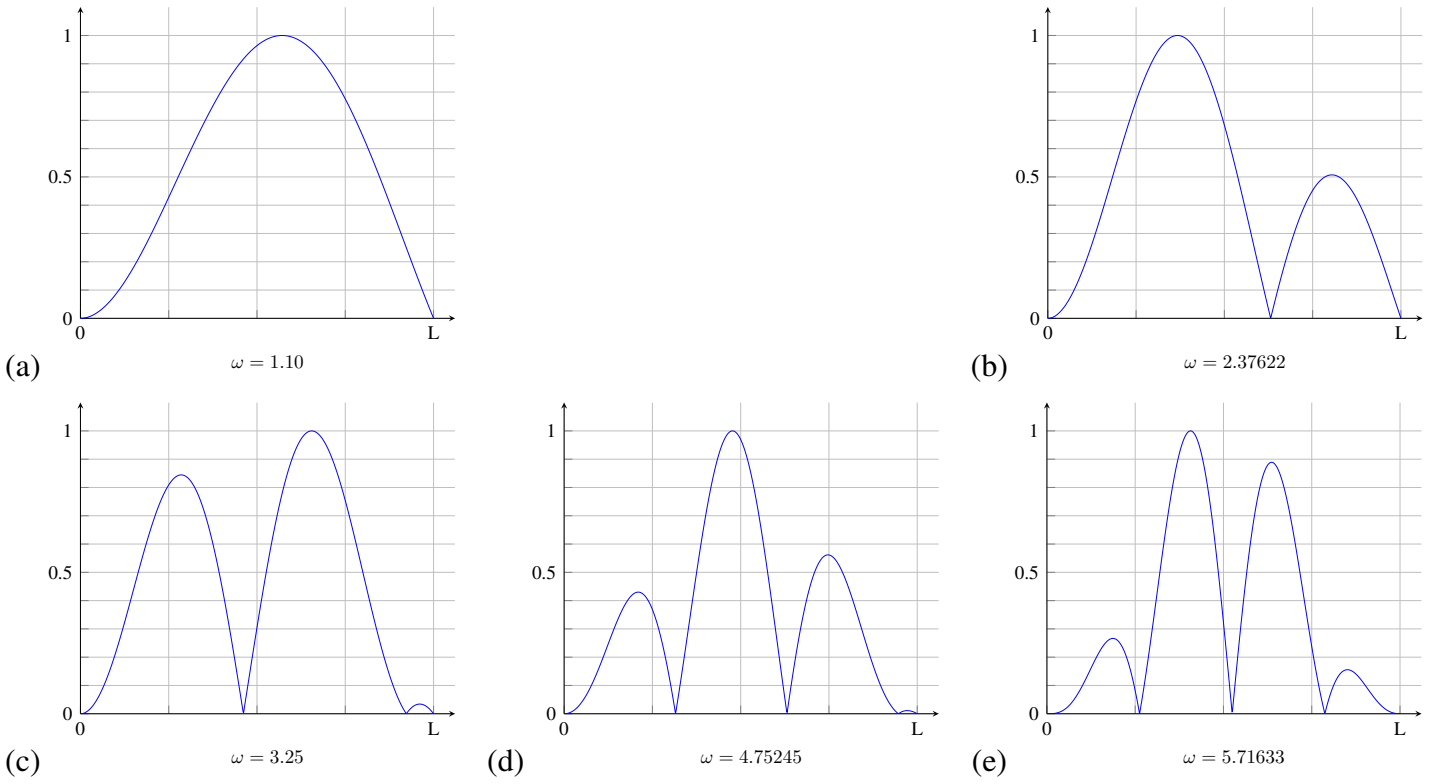

Figure 5: Mode shapes obtained from the technique based on truncated Fourier series for the case when V $= 0$: (a) Mode 1; (b) Mode 2; (c) Mode 3; (d) Mode 4; (e) Mode 5

spotted by Triantafyllou [11]. Moreover the global shape of each solutions are comparable. We can then look at the influence of the velocity on the modes spotted with this method.
Let us consider the system with translating velocity. It is worthwhile to mention that due to translation speed, two traveling waves (with different celerity) are propagating in the cable which is noticeable from the first scale response of the system Eq.(29).
Frequencies obtained for the system with V $\neq 0$ are displayed in Tab.(3). These are sorted with regard to their similarity with the case corresponding to the system without velocity. Still, we can notice that frequencies are approximately decreasing functions of the velocity. The evolution of the modes are depicted in Fig.(6), we see that velocity induces a loss of nodes in the mode shapes and shifts the positions of local maxima and minima from their position corresponding to the system without velocity. The extremum shift tendancy depends on the mode or considered ω. The obtained shapes are similar to those obtained by Triantafyllou [11] but we lose nodes that is a sigificiant difference with the work of Simpson [10].

V (m.s^{-1})	ω_1	ω_2	ω_3	ω_4	ω_5
0	1.10	2.38	3.25	4.75	5.72
7.5	0.996	2.36	3.31	4.51	5.70
10	0.992	2.37	3.31	4.43	5.68
12.5	0.988	2.35	3.56	4.65	5.66
17.5	0.976	2.32	3.51	4.57	5.60
20	0.97	2.19	3.48	4.498	5.57

Table 3: Evolution of the frequencies spotted with the method based on truncated Fourier series ; Precision goal is set as 10^{-3}

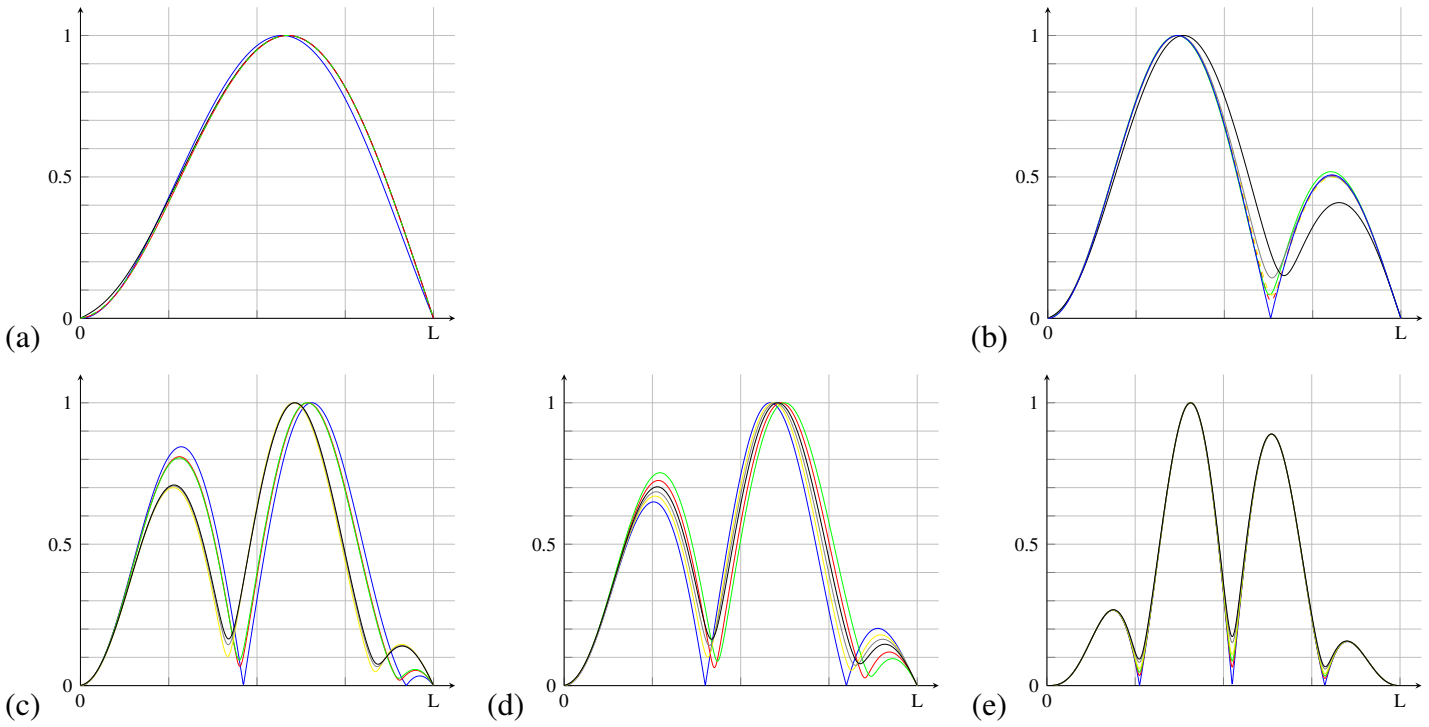

Figure 6: Evolution of the mode obtained as a function of velocity: (—) V $= 0$ m.s^{-1}; (—) V $= 7.5$ m.s^{-1}; (—) V $= 10$ m.s^{-1}; (—) V $= 12.5$ m.s^{-1}; (—) V $= 17.5$ m.s^{-1}; (—) V $= 20$ m.s^{-1}; (a) Mode 1; (b) Mode 2; (c) Mode 3; (d) Mode 4; (e) Mode 5

4.3 Seeking modes via the finite difference method

In this section we seek for the system modes via the numerical scheme named FDM. The linearized dynamics of the cable given by equations (7) and (6) are treated with FDM which is explained in the next section.

4.3.1 A generalized eigenvalue problem

We first assume that the space and time variables are separated as it follows:

$$\hat{p}(s,t) = \mathbf{P}(s)p(t) \tag{67}$$

$$\hat{q}(s,t) = \mathbf{Q}(s)q(t) \tag{68}$$

In this subsection, $(\cdot)'$ and $\dot{(\cdot)}$ respectively refer to space and time derivatives, respectively. The dynamics of the system copies as:

$$\begin{aligned} 0 =& \mathbf{P}\ddot{p} + \left[2V\mathbf{P}'\right]\dot{p} + \left[\left(V^2 - \frac{\mathrm{ES}}{m}\right)\mathbf{P}'' - \frac{\widetilde{T}_\mathrm{S}}{m}(\partial_s\widetilde{\Phi}_\mathrm{S})^2\mathbf{P}\right]p \\ &- \left[2V(\partial_s\widetilde{\Phi}_\mathrm{S})\mathbf{Q}\right]\dot{q} \\ &+ \left[(\partial_s\widetilde{\Phi}_\mathrm{S})\left(\frac{\mathrm{ES} - \widetilde{T}_\mathrm{S}}{m} - V^2\right)\mathbf{Q}' + \left(\frac{\mathrm{ES}}{m} - V^2\right)(\partial_{ss}\widetilde{\Phi}_\mathrm{S})\mathbf{Q}\right]q \end{aligned} \tag{69}$$

and:

$$\begin{aligned}0 =&\mathbf{Q}\ddot{q} + \left[3V\mathbf{Q}'\right]\dot{q} + \left[3V(\partial_s\widetilde{\Phi}_\mathrm{S})\mathbf{P}\right]\dot{p}\\ &+\left[\left(\frac{\mathrm{ES}}{m} - V^2\right)(\partial_s\widetilde{\Phi}_\mathrm{S})^2\mathbf{Q} + \left(2V^2 - \frac{\widetilde{T}_\mathrm{S}}{m}\right)\mathbf{Q}'' - \frac{(\partial_s\widetilde{T}_\mathrm{S})}{m}\mathbf{Q}'\right]q\\ &+\left[(\partial_s\widetilde{\Phi}_\mathrm{S})\left(3V^2 - \frac{\mathrm{ES}+\widetilde{T}_\mathrm{S}}{m}\right)\mathbf{P}'\right]p\\ &-\left[\left((\partial_{ss}\widetilde{\Phi}_\mathrm{S})\left(\frac{\widetilde{T}_\mathrm{S}}{m} - 2V^2\right) + \frac{(\partial_s\widetilde{T}_\mathrm{S})(\partial_s\widetilde{\Phi}_\mathrm{S})}{m}\right)\mathbf{P}\right]p\end{aligned} \tag{70}$$

The domain $s \in [0, L]$ is meshed into N elements. Discrete derivatives are used to compute the relationships between the different cells of the mesh [21]. The dynamics are then described with a vector of length $2N$. For an arbitrary scalar function f:

$$f'(s_k) \approx \frac{f(s_{k+1}) - f(s_{k-1})}{2\Delta s} \tag{71}$$

$$f''(s_k) \approx \frac{f(s_{k+1}) - 2f(s_k) + f(s_{k-1})}{\Delta s^2} \tag{72}$$

$$\text{with } \Delta s = \frac{L}{N+1} \tag{73}$$

By using this meshing strategy on the quantities $\mathbf{P}$, $\mathbf{Q}$, $\widetilde{T}_\mathrm{S}$ and $\widetilde{\Phi}_\mathrm{S}$, a set of $2N$ equations is obtained:

$$\begin{aligned}0 =&Q_k\ddot{q} + \frac{3V\left(Q_{k+1} - Q_{k-1}\right)}{2\Delta\mathrm{s}}\dot{q}\\ &+\frac{Q_k\left(\phi_{k-1} - \phi_{k+1}\right)^2\left(\mathrm{ES} - mV^2\right) - \left(Q_{k-1} - Q_{k+1}\right)\left(T_{k-1} - T_{k+1}\right)}{4\Delta\mathrm{s}^2 m}q\\ &+\frac{\left(Q_{k-1} - 2Q_k + Q_{k+1}\right)\left(2mV^2 - T_k\right)}{\Delta\mathrm{s}^2 m}q + \frac{3VP_k\left(\phi_{k+1} - \phi_{k-1}\right)}{2\Delta\mathrm{s}}\dot{p}\\ &-\frac{\left(P_{k-1} - P_{k+1}\right)\left(\phi_{k-1} - \phi_{k+1}\right)\left(\mathrm{ES} + T_k - 3mV^2\right)}{4\Delta\mathrm{s}^2 m}p\\ &-\frac{P_k\left(T_{k-1} - T_{k+1}\right)\left(\phi_{k-1} - \phi_{k+1}\right)}{4\Delta\mathrm{s}^2 m}p\\ &+\frac{P_k\left(\phi_{k-1} - 2\phi_k + \phi_{k+1}\right)\left(2mV^2 - T_k\right)}{\Delta\mathrm{s}^2 m}p\end{aligned} \tag{74}$$

and:

$$\begin{aligned}0 =&P_k\ddot{p} + \frac{V\left(P_{k+1} - P_{k-1}\right)}{\Delta\mathrm{s}}\dot{p} + \frac{VQ_k\left(\phi_{k-1} - \phi_{k+1}\right)}{\Delta\mathrm{s}}\dot{q}\\ &-\frac{\left(P_{k-1} - 2P_k + P_{k+1}\right)\left(\mathrm{ES} - mV^2\right)}{\Delta\mathrm{s}^2 m}p - \frac{P_kT_k\left(\phi_{k-1} - \phi_{k+1}\right)^2}{4\Delta\mathrm{s}^2 m}p\\ &+\frac{\left(Q_{k-1} - Q_{k+1}\right)\left(\phi_{k-1} - \phi_{k+1}\right)\left(\mathrm{ES} - T_k - mV^2\right)}{4\Delta\mathrm{s}^2 m}q\\ &+\frac{Q_k\left(\phi_{k-1} - 2\phi_k + \phi_{k+1}\right)\left(\mathrm{ES} - mV^2\right)}{\Delta\mathrm{s}^2 m}q\end{aligned} \tag{75}$$

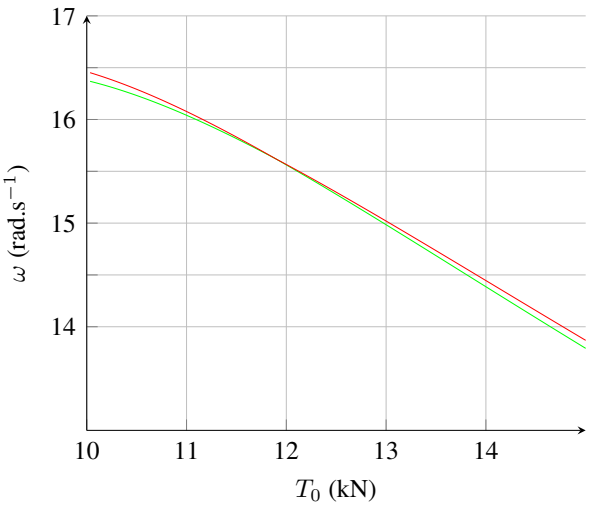

Figure 7: Veering phenomenon obtained between second and third mode via FDM

where f_k accounts for the value of the scalar function f at point $s = k\Delta s$ with $k \in [1, N] \cap \mathbb{N}$. For presenting the problem in a canonical form, a variable X is defined as follows:

$$X(t) = \begin{pmatrix} P_1 p(t) \\ \vdots \\ P_N p(t) \\ Q_1 p(t) \\ \vdots \\ Q_N p(t) \end{pmatrix} \tag{76}$$

Boundary conditions can be applied by considering that:

$$P_0 = P_{N+1} = Q_0 = Q_{N+1} = 0 \tag{77}$$

Periodic solutions can be computed as the solutions of a generalized eigenvalue problem as explained in reference [22]:

$$\underline{\underline{\delta}}\ddot{X} + \underline{\underline{C}}\dot{X} + \underline{\underline{K}}X = 0 \tag{78}$$

Let us define the vector Y vector as:

$$Y = \begin{pmatrix} X \\ \dot{X} \end{pmatrix} \tag{79}$$

Then the eigenvalue problem reads:

$$\dot{Y} - \begin{pmatrix} \underline{\underline{\delta}} & \underline{\underline{0}} \\ -\underline{\underline{C}} & -\underline{\underline{K}} \end{pmatrix} Y = 0 \tag{80}$$

The modes of the system are obtained by solving the next problem in ω:

$$\left(\begin{pmatrix} \underline{\underline{\delta}} & \underline{\underline{0}} \\ -\underline{\underline{C}} & -\underline{\underline{K}} \end{pmatrix} - i\omega \underline{\underline{\delta}} \right) Y = 0 \tag{81}$$

where $\underline{\underline{\delta}}$ is the unity matrix of dimension $2N$.
This numerical method allows to catch complex eigenvalues of translating cable. In this configuration, detected modes are complex conjugate. This approach seems to be more reliable than the Fourier series approach. Mode veering phenomena [23] is spotted for low tensions and asymptotically gives real modes when the velocity tends to zero. The veering phenomena is shown via the finite difference method allows to validate the approximation done in the pseudo-analytical approach when the ration of self-weight by tension is sufficiently small.

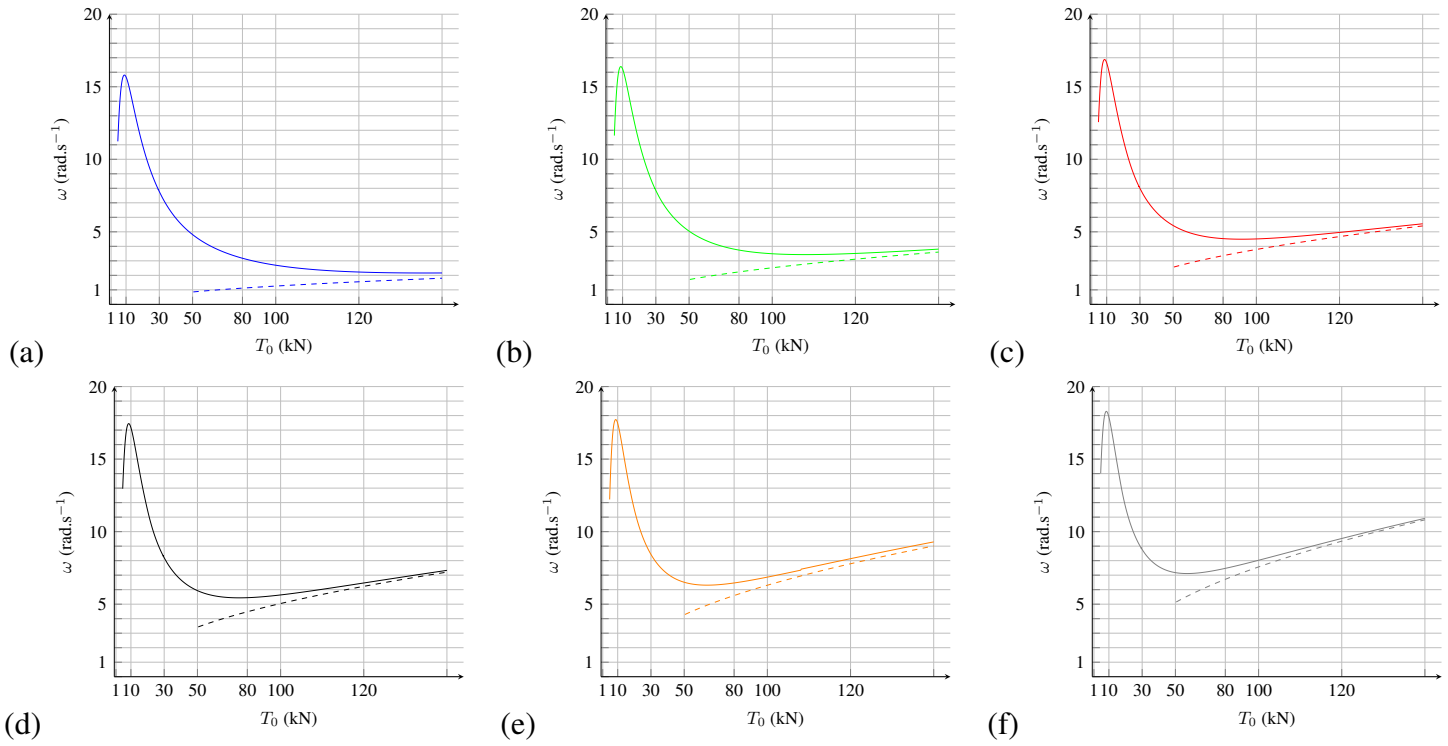

Figure 8: Frequency versus initial tension of the cable obtained by numerical computation via FDM (solid line) and analytical prediction via SMSM (dashed line); (a) 1st mode - (b) 2nd mode - (c) 3rd mode - (d) 4th mode - (e) 5th mode - (f) 6th mode

4.3.2 Comparison between obtained results by FDM and Fourier series

The results of mode computation with FDM and the SMSM are presented in Fig.(8). We see that the Fourier series approach provides insight about the modal characteristics of the system when the tension becomes sufficiently big with regards to the self-weight effects as depicted in Fig.(8). For this reason, the detected solutions are not acceptable for sagged cables. More developments are needed to effectively detect the natural frequencies of a translating cable. The obtained mode shapes for the same set of parameters used for Fig.(2) are depicted in Fig.(9).

5 Conclusions

Different techniques are proposed to trace modal characteristics of translating cables. After separation of spatio-temporal variables of system equations, a space multiple scale method is used to treat equations in space. It is found that some modes can be derived via both analytical and analytical-numerical methods. The first approach provides suitable tools for having deeper insight on the influence of the translation speed on modal responses of the system. The latter technique provides a reliable tool to detect systems frequencies apart from some difficulties in finding roots of the characteristic equation. In both cases, complex mode shapes can be obtained and the detected frequencies seem to be more accurate when the system gets closer to a taut cable condition. Results are confronted with those which are obtained by finite difference technique showing a coherence between different methods. As perspectives of this work, we will consider extensibility on the stationary responses of the multi-span translating cable. Then, the dynamics of the system around the stationary position will be revealed by an adapted and developed finite element method taking into account the effect of the pylons and realistic boundary and continuity conditions.

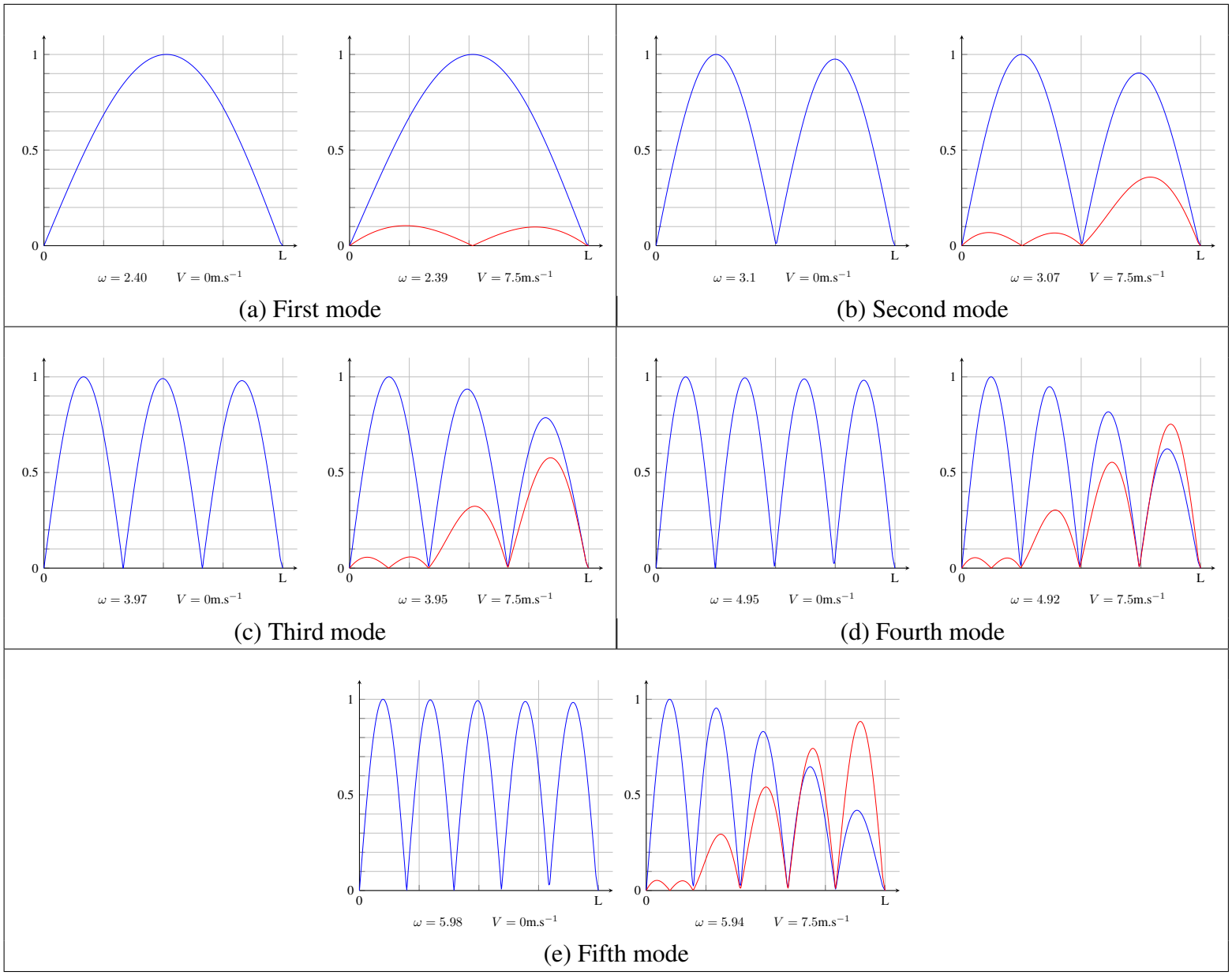

Figure 9: Absolute value of the real (—) and the imaginary (—) parts of the first five modes obtained from FDM

Method	ω_1	ω_2	ω_3	ω_4	ω_5
Current work					
SMSM	1.21	2.43	3.64	4.85	6.07
Fourier	1.10	2.38	3.25	4.75	5.72
FDM	2.40	3.1	3.98	4.97	6.01
Comparison					
Irvine [1]	2.17	2.20	3.39	4.39	5.51
Triantafyllou [20]	2.15	2.21	3.38	4.37	5.48

Table 4: Detected solution via the technique based on truncated Fourier series with an error tolerance of 10^{-12} with a varying N and V $= 0$ compared to the frequencies obtained earlier by Irvine [1] and Triantafyllou [20]

Acknowledgments

The authors thank the following organizations for supporting this research:

- The *Ministère de la transition écologique et solidaire* especially its service named as "STRMTG".
- LABEX CELYA (ANR-10-LABX-0060) of the *Université de Lyon* within the program "Investissement d?Avenir" (ANR-11-IDEX-0007) operated by the French National Research Agency (ANR).

References

[1] H. M. Irvine, Cable structures (1992) no. of pages: 259, Earthquake Engng. Struct. Dyn.doi:10.1002/eqe.4290100213.

[2] V. Gattulli, F. Di Fabio, A. Luongo, "Simple and double Hopf bifurcations in aeroelastic oscillators with Tuned Mass Dampers", *Journal of The Franklin Institute* 338 (2-3) (2001) 187–201.

[3] F. Treyssede, "Free linear vibrations of cables under thermal stress", *Journal of Sound and Vibration* 327 (1-2) (2009) 1–8.

[4] A. Sofi, G. Muscolino, "Dynamic analysis of suspended cables carrying moving oscillators", *International Journal of Solids and Structures* 44 (21) (2007) 6725–6743.

[5] V. Gattulli, M. Lepidi, F. Potenza, U. Di Sabatino, Dynamics of masonry walls connected by a vibrating cable in a historic structure, Meccanica 51 (2016) 2813–2826.

[6] V. Gattulli, M. Lepidi, F. Potenza, U. Di Sabatino, Modal interactions in the nonlinear dynamics of a beam–cable–beam, Nonlinear Dynamics 96 (4) (2019) 2547–2566.

[7] G. Rega, "Nonlinear vibrations of suspended cables Part I: Modeling and analysis", *Applied Mechanics Reviews* 57 (6) (2004) 443.

[8] W. Lacarbonara, The Elastic Cable: From Formulation to Computation, 2013.

[9] R. Skutch, "Uber die bewegung eines gespannten fadens, welcher gezwungen ist, durch zwei feste punkte, mit einer constanten geshwindigkeit zu gehen, und zwischen denselben in transversal-schwingungen von geriger amplitude versetzt wird", *Annalen der Physik und Chemie* 297 (5) (1897).

[10] A. Simpson, "On the oscillatory motions of translating elastic cables", *Journal of sound and vibrations* 20 (2) (1972) 177–189.

[11] M. Triantafyllou, "The dynamics of translating cables", *Journal of Sound and Vibration* 103 (2) (1985) 171–182.

[12] N. I. Zhirnov, On the nature of the genralized WKB method, *Soviet Physics Journal* (1966) 25–28.

[13] O. M. O'Reilly, P. Varadi, "Elastic equilibria of translating cables", *Acta Mechanica* 108 (1995) 189–206.

[14] N. V. Gaiko, W. T. van Horssen, "On transversal oscillations of a vertically translating string with small time-harmonic length variations", *Journal of Sound Vibration* 383 (2016) 339–348.

[15] N. V. Gaiko, "Transversal waves and vibrations in axially moving continua" - PhD Thesis - TU Delft University of Technology, 2017.

[16] J. Warminski, D. Zulli, J. Rega, G.and Latalski, Revisited modelling and multimodal nonlinear oscillations of a sagged cable under support motion, Meccanica 51 (2016) 2541–2575.

[17] M. Ferretti, D. Zulli, A. Luongo, A continuum approach to the nonlinear in-plane galloping of shallow flexible cables, Advances in Mathematical Physics 2019 (2019).

[18] A. H. Nayfeh, D. Mook, "Nonlinear Oscillations", Wiley-VCH Verlag GmbH, 1995.

[19] R. L. Herman, A second course in ordinary differential equations: Dynamical Systems and Boundary value problems, 2008.

[20] M. Triantafyllou, "The dynamics of taut inclined cables", *The Quarterly Journal of Mechanics and Applied Mathematics* 37 (3) (1984) 421–440.

[21] M. Davis, Lecture notes: Finite difference methods, Course in mathematics and finance, *Imperial College London* (2010).

[22] G. Lallement, D. J. Inman, "A tutorial on complex eigenvalues", *Proceedings of the 13th International Modal Analysis Conference* (1995) 490–495.

[23] C. Pierre, "Mode localization and eigenvalue loci veering phenomena in disordered structures", *Journal of Sound and Vibrations* (1988) 485–502.

A α_i coefficients

$$
\begin{aligned}
\alpha_1 =& \frac{1}{2}a_1^2 L^2 \widetilde{\xi}_1 \omega^2 - i a_1 L \widetilde{\xi}_1 \omega + \frac{i\gamma_1 e^{i\Omega_1 s_1}\left(2b_1 \widetilde{T}_a \Omega_1\right)}{(a_1-b_1)} \\
& - \frac{i b_1 \gamma_1 e^{i(-a_1 L\omega + b_1 L\omega + \Omega_1 s_1)}\left(b_1^2(-L)\widetilde{\xi}_1\omega + 2b_1 m \mathrm{V}^2 \Omega_1 + 2m\mathrm{V}\Omega_1\right)}{(a_1-b_1)^2} \\
& - \frac{i\gamma_1 e^{i\Omega_1 s_1}\left(a_1\left(2b_1 m\mathrm{V}^2\Omega_1 + i b_1 \widetilde{\xi}_1 + 2m\mathrm{V}\Omega_1\right)\right)}{(a_1-b_1)^2} \\
& + \frac{i\gamma_1 e^{i\Omega_1 s_1}\left(2b_1 m\mathrm{V}\Omega_1(b_1\mathrm{V}+1)\right)}{(a_1-b_1)^2} - \frac{\gamma_1 e^{i(-a_1 L\omega + b_1 L\omega + \Omega_1 s_1)} a_1 b_1 \widetilde{\xi}_1}{(a_1-b_1)^2} \\
& - \frac{i\gamma_1 e^{i(-a_1 L\omega + b_1 L\omega + \Omega_1 s_1)}\left(a_1\left(b_1^2 L\widetilde{\xi}_1\omega - 2b_1 m\mathrm{V}^2\Omega_1 - 2m\mathrm{V}\Omega_1\right)\right)}{(a_1-b_1)^2} \\
& - \frac{i\gamma_1 e^{i(-a_1 L\omega + b_1 L\omega + \Omega_1 s_1)}\left(2b_1 \widetilde{T}_a \Omega_1 (a_1-b_1)\right)}{(a_1-b_1)^2}
\end{aligned} \tag{82}
$$

$$
\begin{aligned}
\alpha_2 =& \frac{2\gamma_1\left(m\mathrm{V}(b_1\mathrm{V}+1) - b_1\widetilde{T}_a\right)e^{i(-a_1 L\omega + b_1 L\omega + \Omega_1 s_1)}}{a_1-b_1} \\
& - \frac{2\gamma_1 e^{i\Omega_1 s_1}\left(m\mathrm{V}(b_1\mathrm{V}+1) - b_1\widetilde{T}_a\right)}{a_1-b_1} \\
& + 2i a_1 L m\mathrm{V}^2\omega - 2i a_1 L\widetilde{T}_a\omega + 2iLm\mathrm{V}\omega
\end{aligned} \tag{83}
$$

$$
\begin{aligned}
\alpha_3 =& \frac{\gamma_1 L\omega e^{i s_1\Omega_1}}{2}\left(b_1^2(-L)\widetilde{\xi}_1\omega + 4b_1 m\mathrm{V}^2\Omega_1 + 2ib_1\widetilde{\xi}_1 + 4m\mathrm{V}\Omega_1\right) \\
& + \frac{2a_1 b_1 \widetilde{\xi}_1\left(-1 + e^{iL\omega(a_1-b_1)}\right)}{2(a_1-b_1)^2} - 2b_1\gamma_1 L\widetilde{T}_a\omega\Omega_1 e^{i\Omega_1 s_1} \\
& \frac{-2ia_1^3 L\widetilde{\xi}_1\omega e^{iL\omega(a_1-b_1)} + 2ia_1^2 b_1 L\widetilde{\xi}_1\omega e^{iL\omega(a_1-b_1)}}{2(a_1-b_1)^2}
\end{aligned} \tag{84}
$$

$$
\begin{aligned}
\alpha_4 =& 2m\mathrm{V}i\gamma_1 L\omega(b_1\mathrm{V}+1)e^{i s_1\Omega_1} \\
& + \frac{2\left(m\mathrm{V}\left(a_1\mathrm{V}+1-(a_1\mathrm{V}+1)e^{iL\omega(a_1-b_1)}\right)\right)}{a_1-b_1} \\
& + \frac{2\left(-\widetilde{T}_a\left(ib_1\gamma_1 L\omega(a_1-b_1)e^{i\Omega_1 s_1} + a_1\left(-e^{iL\omega(a_1-b_1)}\right) + a_1\right)\right)}{a_1-b_1}
\end{aligned} \tag{85}
$$

B Π, Σ, Δ and Γ coefficients

$$\begin{aligned}\Sigma =&\frac{2e^{-iL\omega(a_1+b_1)}b_1(a_1L\omega+i)e^{iL\omega(a_1+b_1)}\left(m\mathrm{V}(a_1\mathrm{V}+1)-a_1\widetilde{T}_a\right)}{a_1b_1\omega(a_1-b_1)}\\&+\frac{2e^{-iL\omega(a_1+b_1)}b_1e^{ia_1L\omega}(-a_1L\omega+i)\left(m\mathrm{V}(a_1\mathrm{V}+1)-a_1\widetilde{T}_a\right)}{a_1b_1\omega(a_1-b_1)}\\&-\frac{2e^{-iL\omega(a_1+b_1)}b_1\left(ie^{2ia_1L\omega}+ie^{ib_1L\omega}\right)\left(m\mathrm{V}(a_1\mathrm{V}+1)-a_1\widetilde{T}_a\right)}{a_1b_1\omega(a_1-b_1)}\\&-\frac{2e^{-iL\omega(a_1+b_1)}a_1^2L\omega e^{ia_1L\omega}\left(-1+e^{ib_1L\omega}\right)\left(m\mathrm{V}(a_1\mathrm{V}+1)-a_1\widetilde{T}_a\right)}{a_1b_1\omega(a_1-b_1)}\end{aligned} \tag{86}$$

$$\begin{aligned}\Gamma =&\frac{2\gamma_1e^{-iL\omega(a_1+b_1)}b_1^2L\omega\left(-1+e^{ia_1L\omega}\right)e^{ib_1L\omega}\left(m\mathrm{V}(b_1\mathrm{V}+1)-b_1\widetilde{T}_a\right)}{a_1b_1\omega(a_1-b_1)}\\&+\frac{2\gamma_1e^{-iL\omega(a_1+b_1)}a_1\left(b_1L\omega+i\right)e^{iL\omega(a_1+b_1)}\left(m\mathrm{V}(b_1\mathrm{V}+1)-b_1\widetilde{T}_a\right)}{a_1b_1\omega(a_1-b_1)}\\&+\frac{2\gamma_1e^{-iL\omega(a_1+b_1)}\left(e^{ib_1L\omega}(b_1L\omega-i)\right)\left(m\mathrm{V}(b_1\mathrm{V}+1)-b_1\widetilde{T}_a\right)}{b_1\omega(a_1-b_1)}\\&+\frac{2\gamma_1e^{-iL\omega(a_1+b_1)}\left(ie^{ia_1L\omega}+ie^{2ib_1L\omega}\right)\left(m\mathrm{V}(b_1\mathrm{V}+1)-b_1\widetilde{T}_a\right)}{b_1\omega(a_1-b_1)}\end{aligned} \tag{87}$$

$$\begin{aligned}\Pi =&\frac{\xi_1e^{-iL\omega(a_1+b_1)}\left(a_1^3L\omega e^{ia_1L\omega}(2+ia_1L\omega)\left(-1+e^{ib_1L\omega}\right)\right)}{2b_1\omega(a_1-b_1)^2}\\&\frac{\xi_1e^{-iL\omega(a_1+b_1)}\left(b_1^2\left(ia_1^2L^2\omega^2+2a_1L\omega+2i\right)e^{iL\omega(a_1+b_1)}\right)}{2b_1\omega(a_1-b_1)^2}\\&+\frac{\xi_1e^{-iL\omega(a_1+b_1)}\left(b_1^2\left(e^{ia_1L\omega}\left(-ia_1^2L^2\omega^2-4a_1L\omega+2i\right)\right)\right)}{2b_1\omega(a_1-b_1)^2}\\&+\frac{\xi_1e^{-iL\omega(a_1+b_1)}\left(b_1^2\left(2e^{2ia_1L\omega}(a_1L\omega-i)-2ie^{ib_1L\omega}\right)\right)}{2b_1\omega(a_1-b_1)^2}\\&-\frac{a_1^2L\xi_1e^{-iL\omega(a_1+b_1)}\left((2+ia_1L\omega)e^{ib_1L\omega}\right)e^{ia_1L\omega}}{(a_1-b_1)^2}\\&+\frac{a_1^2L\xi_1e^{-iL\omega(a_1+b_1)}\left(ia_1L\omega-e^{ia_1L\omega}+3\right)e^{ia_1L\omega}}{(a_1-b_1)^2}\\&-\frac{\xi_1e^{-iL\omega(a_1+b_1)}a_1^2Le^{ia_1L\omega}\left((2+ia_1L\omega)e^{ib_1L\omega}\right)}{(a_1-b_1)^2}\\&+\frac{\xi_1e^{-iL\omega(a_1+b_1)}a_1^2Le^{ia_1L\omega}\left(ia_1L\omega-e^{ia_1L\omega}+3\right)}{(a_1-b_1)^2}\end{aligned} \tag{88}$$

$$
\begin{aligned}
\Delta =& \frac{\gamma_1 e^{-iL\omega(a_1+b_1)} 2a_1^2 m\mathrm{V}(b_1\mathrm{V}+1)\left((1-ib_1L\omega)e^{iL\omega(a_1+b_1)}-e^{ia_1L\omega}\right)}{b_1(a_1-b_1)^2} \\
& \frac{\gamma_1 e^{-iL\omega(a_1+b_1)} 2a_1^2 m\mathrm{V}(b_1\mathrm{V}+1)\left(-e^{2ib_1L\omega}+e^{ib_1L\omega}(1+ib_1L\omega)\right)}{b_1(a_1-b_1)^2} \\
& + \frac{\gamma_1 e^{-iL\omega(a_1+b_1)} a_1\left(e^{ia_1L\omega}(8m\mathrm{V}\omega(b_1\mathrm{V}+1)-2i\widetilde{\xi}_1)\right)}{2\omega(a_1-b_1)^2} \\
& + \frac{\gamma_1 e^{-iL\omega(a_1+b_1)} a_1\left(e^{iL\omega(a_1+b_1)}(4m\mathrm{V}\omega(b_1\mathrm{V}+1)(-2+3ib_1L\omega)\right)}{2\omega(a_1-b_1)^2} \\
& + \frac{\gamma_1 e^{-iL\omega(a_1+b_1)} a_1\left(e^{iL\omega(a_1+b_1)}\widetilde{\xi}_1(b_1L\omega(2+ib_1L\omega)+2i)\right)}{2\omega(a_1-b_1)^2} \\
& + \frac{\gamma_1 e^{-iL\omega(a_1+b_1)} a_1\left(2e^{2ib_1L\omega}(4m\mathrm{V}\omega(b_1\mathrm{V}+1)+\widetilde{\xi}_1(b_1L\omega-i))\right)}{2\omega(a_1-b_1)^2} \\
& + \frac{\gamma_1 e^{-iL\omega(a_1+b_1)} a_1\left(-ie^{ib_1L\omega}4m\mathrm{V}\omega(b_1\mathrm{V}+1)(3b_1L\omega-2i)\right)}{2\omega(a_1-b_1)^2} \\
& + \frac{\gamma_1 e^{-iL\omega(a_1+b_1)} a_1\left(\widetilde{\xi}_1(-2+b_1L\omega(b_1L\omega-4i))\right)}{2\omega(a_1-b_1)^2} \\
& + \frac{\gamma_1 e^{-iL\omega(a_1+b_1)}\left(b_1^3L\left(-1+e^{ia_1L\omega}\right)e^{ib_1L\omega}(2\widetilde{\xi}_1+i\omega(b_1L\widetilde{\xi}_1))\right)}{2a_1(a_1-b_1)^2} \\
& + \frac{\gamma_1 e^{-iL\omega(a_1+b_1)}\left(b_1^3L\left(-1+e^{ia_1L\omega}\right)e^{ib_1L\omega}(i\omega(4m\mathrm{V}(b_1\mathrm{V}+1)))\right)}{2a_1(a_1-b_1)^2} \\
& + \frac{\gamma_1 e^{-iL\omega(a_1+b_1)}\left(b_1\left(e^{iL\omega(a_1+b_1)}(2m\mathrm{V}(b_1\mathrm{V}+1)(1-3ib_1L\omega))\right)\right)}{(a_1-b_1)^2} \\
& + \frac{\gamma_1 e^{-iL\omega(a_1+b_1)}\left(b_1\left(e^{iL\omega(a_1+b_1)}(b_1L\widetilde{\xi}_1(-2-ib_1L\omega))\right)\right)}{(a_1-b_1)^2} \\
& - \frac{\gamma_1 e^{-iL\omega(a_1+b_1)}\left(b_1\left(2m\mathrm{V}(b_1\mathrm{V}+1)e^{ia_1L\omega}\right)\right)}{(a_1-b_1)^2} \\
& - \frac{\gamma_1 e^{-iL\omega(a_1+b_1)}\left(b_1\left(e^{2ib_1L\omega}(b_1L\widetilde{\xi}_1+2m\mathrm{V}(b_1\mathrm{V}+1))\right)\right)}{(a_1-b_1)^2} \\
& + \frac{\gamma_1 e^{-iL\omega(a_1+b_1)}\left(b_1\left(e^{ib_1L\omega}(2m\mathrm{V}(b_1\mathrm{V}+1)(1+3ib_1L\omega))\right)\right)}{(a_1-b_1)^2} \\
& + \frac{\gamma_1 e^{-iL\omega(a_1+b_1)}\left(b_1\left(e^{ib_1L\omega}(b_1L\widetilde{\xi}_1(3+ib_1L\omega))\right)\right)}{(a_1-b_1)^2} \\
& + \gamma_1 e^{-iL\omega(a_1+b_1)}\left(2\widetilde{T}_a\left(\left((-1+ib_1L\omega)e^{iL\omega(a_1+b_1)}+e^{ia_1L\omega}\right)\right)\right) \\
& + \gamma_1 e^{-iL\omega(a_1+b_1)}\left(2\widetilde{T}_a\left(\left(e^{ib_1L\omega}(-1-ib_1L\omega)+e^{2ib_1L\omega}\right)\right)\right) \\
& + \frac{\gamma_1 e^{-iL\omega(a_1+b_1)}\left(2\widetilde{T}_a\left(-ib_1^2L\omega\left(-1+e^{ia_1L\omega}\right)e^{ib_1L\omega}\right)\right)}{a_1}
\end{aligned}
\tag{89}
$$